Nuclear Science and Techniques **24** (2013) 050525

Mean-field effects on matter and antimatter elliptic flow

KO Cheming[1,*] CHEN Liewen[2] GRECO Vincenzo[3] LI Feng[1] LIN Ziwei[4]
PLUMARI Salvatore[3] SONG Taesoo[1] XU Jun[5]

[1]*Cyclotron Institute and Department of Physics and Astronomy, Texas A&M University, College Station, TX 77843, USA*

[2]*Department of Physics, Shanghai Jiao Tong University, Shanghai 200240, China*

[3]*Dipartimento di Fisica e Astronomia, Universitá di Catania, Via S. Sofia 64, 95125 Catania, Italy*

[4]*Department of Physics, East Carolina University, C-209 Howell Science Complex, Greenville, NC 27858, USA*

[5]*Shanghai Institute of Applied Physics, Chinese Academy of Sciences, Shanghai 201800, China*

Abstract We report our recent work on mean-field potential effects on the elliptic flows of matters and antimatters in heavy ion collisions leading to the production of a baryon-rich matter. Within the framework of a multiphase transport (AMPT) model that includes both initial partonic and final hadronic interactions, we have found that including mean-field potentials in the hadronic phase leads to a splitting of the elliptic flows of particles and their antiparticles, providing thus a plausible explanation of the different elliptic flows between p and anti-p, K^+ and K^-, and π^+ and π^- observed by the STAR Collaboration in the Beam Energy Scan (BES) program at the Relativistic Heavy Ion Collider (RHIC). Using a partonic transport model based on the Nambu-Jona-Lasinio (NJL) model, we have also studied the effect of scalar and vector mean fields on the elliptic flows of quarks and antiquarks in these collisions. Converting quarks and antiquarks at hadronization to hadrons via the quark coalescence model, we have found that the elliptic flow differences between particles and antiparticles also depend on the strength of the quark vector coupling in baryon-rich quark-gluon plasma, providing thus the possibility of extracting information on the latter's properties from the BES program at RHIC.

Key words Relativistic heavy ion collisions, Hadronic and partonic mean fields, Elliptic flows

1 Introduction

Heavy ion collisions at relativistic energies provide the possibility to study the phase structure of the strongly interacting matter that is described by the quantum chromodynamics (QCD). For the top energy available at RHIC and at the Large Hadron Collider (LHC), the produced quark-gluon plasma (QGP) is nearly baryon free and thus has very small baryon chemical potentials. According to lattice QCD calculations[1-3], the transition from the QGP phase to the hadronic matter (HM) phase in this region of the phase diagram is a smooth crossover without a clear phase boundary. The phase transition between QGP and HM is expected to change from the crossover to a first-order transition at a certain finite baryon chemical potential called the critical point in the QCD phase diagram[4-7]. To probe this region of the QCD phase diagram, the BES program of Au+Au collisions at much lower center mass energies of 7.7 GeV, 11.5 GeV and 39 GeV than the top energy has recently been carried out at RHIC by the STAR Collaboration[8,9]. Although no definitive signals for a first-order phase transition and the critical end point have been established, a number of interesting results have been observed[9]. One of them is the increasing difference between the elliptic flows of particles and antiparticles, thus a breaking of the number of constituent quark number scaling of elliptic

Supported by the U.S. National Science Foundation (Grant No.PHY-106857), the Welch Foundation (Grant No.A-1358), the NNSF of China (Grant Nos.11135011 and 11275125), Shanghai Rising-Star Program (Grant No.11QH1401100), "Shu Guang" project and "Eastern Scholar" program of Shanghai, and the ERC-StG (Grant QGPDyn No.259684).

* Corresponding author. *E-mail address:* ko@comp.tamu.edu

Received date: 2013-06-27

flows, as the collision energy decreases. Such a behavior cannot be described by a simple hydrodynamic or hadronic cascade model even if the quark coalescence is considered during the hadronization of produced QGP[10]. Several theoretical attempts have been made to explain this surprising and interesting experimental result. These include the different elliptic flows of transported and produced partons during the initial stage of heavy ion collisions[11]; the chiral magnetic effect induced by the strong magnetic field in non-central heavy ion collisions[12], the hadronic[13] and the partonic[14] mean-field effects, and the local thermal and baryon chemical equilibrium effect[15]. In the present talk, we review the results on the mean-field effects on the elliptic flows of particles and antiparticles in heavy ion collisions at BES energies.

2 Hadronic mean-field potentials and elliptic flows

In Ref.[13], we have studied quantitatively the elliptic flows of particles and their antiparticles at BES energies by extending the AMPT model[16] to include the potentials of baryons, kaons, and pions as well as their antiparticles. The AMPT model is a hybrid model with the initial particle distributions generated by the Heavy-Ion Jet Interaction Generator (HIJING) model[17] via the Lund string fragmentation model. In the string melting version of the AMPT model, which is used in Ref.[13], hadrons produced from excited strings in the HIJING model are converted to their valence quarks and antiquarks, and their evolution in time and space is then modeled by Zhang's parton cascade (ZPC) model[18]. Different from previous applications of the AMPT model for heavy ion collisions at higher energies, the parton scattering cross section and the ending time of the partonic stage are adjusted in Ref.[13] to approximately reproduce measured elliptic flows and the hadronic energy density (~0.30–0.35 GeV/fm^3) at the extracted baryon chemical potential and temperature at chemical freeze out using the statistical model[19]. Specifically, the parton scattering cross section is taken to be isotropic with the values 3 mb, 6 mb and 10 mb and the ending times of the partonic stage to be 3.5 fm/c, 2.6 fm/c and 2.9 fm/c for collisions at the center of mass energies of 7.7 GeV, 11.5 GeV and 39 GeV, respectively. At hadronization, quarks and antiquarks in the AMPT model are converted to hadrons via a spatial coalescence model, and the scatterings between hadrons in the hadronic stage are described by a relativistic transport (ART) model[20] that has been extended to also include particle-antiparticle annihilations and their inverse reactions.

2.1 Hadronic potentials

It is known from heavy ion collisions at lower collision energies at SIS/GSI and AGS/BNL that the elliptic flow of nucleons is affected not only by their scattering but also by their mean-field potentials in the hadronic matter[21]. This is because particles with attractive potentials are more likely to be trapped in the system and move in the direction perpendicular to the participant plane while those with repulsive potentials are more likely to leave the system and move along the participant plane, thus reducing and enhancing their respective elliptic flows. Also, the potentials of a particle and its antiparticle are different, and they generally have opposite signs at high densities[22,23]. As a result, particles and antiparticles are expected to have different elliptic flows in heavy ion collisions when the produced matter has a nonzero baryon chemical potential. Furthermore, the difference between the potentials of a particle and its antiparticle diminishes with decreasing baryon chemical potential, so their elliptic flows are expected to become similar in higher energy collisions when more antiparticles are produced. These effects are all consistent with what have been seen in the experimental data from the BES program.

For the nucleon and antinucleon potentials, we take them from the relativistic mean-field model used in the Relativistic Vlasov-Uehling-Uhlenbeck transport model[24] in terms of the nucleon scalar and vector self-energies in a hadronic matter. Because of the G-parity, nucleons and antinucleons contribute both positively to the scalar self-energy but positively and negatively to the vector self-energy, respectively. Since only the light quarks in baryons and antibaryons contribute to the scalar and vector self-energies in the mean-field approach, the potentials of strange baryons

and antibaryons are reduced relative to those of nucleons and antinucleons according to the ratios of their light quark numbers. For the kaon and antikaon potentials in nuclear medium, they are also taken from Refs.[24,25] based on the chiral effective Lagrangian that fits the empirical data on kaon- and antikaon-nucleus scattering. The resulting potential is then repulsive for a kaon and attractive for an antikaon. The pion potentials are related to their self-energies and have been calculated in Ref.[26] from the pion-nucleon *s*-wave interaction up to the two-loop order in chiral perturbation theory. In asymmetric nuclear matter, this leads to a splitting of the mean-field potentials for positively and negatively charged pions.

In the absence of antibaryons, the nucleon potential is slightly attractive while that of antinucleon is strongly attractive, with values of about –60 MeV and –260 MeV, respectively, at normal nuclear matter density ρ_0=0.16 fm^{-3}. The latter is similar to that determined from the non-linear derivative model for small antinucleon kinetic energies[27] and is also consistent with those extrapolated from experimental data on antiproton atoms[28-33]. In antibaryon-free matter, the K^+ potential is slightly repulsive while the K^- potential is deeply attractive, and their values at ρ_0 are about 20 MeV and –120 MeV, respectively, similar to those extracted from experimental data[34-37] and used in the previous study[38]. For pions in neutron-rich nuclear matter, the potential is weakly repulsive and attractive for π^- and π^+, respectively, and the strength at ρ_0 and isospin asymmetry $\delta=(\rho_n-\rho_p)/(\rho_n+\rho_p)$=0.2 is about 14 MeV for π^- and –1 MeV for π^+[26].

2.2 Particle and antiparticle elliptic flows

The differential elliptic flows of p, K^+, and π^- as well as their antiparticles with respect to the participant plane with and without hadronic potentials at three different BES energies from the string melting AMPT model are shown in Fig.1. Without hadronic potentials elliptic flows from the AMPT model are similar for particles and their antiparticles, including hadronic potentials which slightly increases the p and anti-p elliptic flows at p_T<0.5 GeV/c, while reduces slightly (strongly) the p (anti-p) elliptic flow at higher p_T. Hadronic potentials also increase slightly the elliptic flows of K^+ while mostly reduce that of K^-. In addition, the effect from potentials on the elliptic flow decreases with increasing collision energy, which is consistent with the decreasing net baryon density of produced hadronic matter with increasing collision energy. The difference between the differential elliptic flows of p and anti-p, and between those of K^+ and K^- below collision energy of 11.5 GeV are qualitatively consistent with experimental data[9], while that of π^- and π^+ is small in all three energies due to the small isospin asymmetries of produced matter.

Our results for the relative p_T-integrated v_2 difference between particles and their antiparticles, defined by $[v_2(P)–v_2(\text{anti-}P)]/v_2(P)$, with and without hadronic potentials are shown in Fig.2. These differences are very small in the absence of hadronic potentials, including hadronic potentials increases the relative v_2 difference between p and anti-p and between K^+ and K^- up to about 30% at 7.7 GeV and 20% at 11.5 GeV but negligibly at 39 GeV. These results are qualitatively consistent with the measured values of about 63% and 13% at 7.7 GeV, 44% and 3% at 11.5 GeV, and 12% and 1% for the relative v_2 difference between p and anti-p and between K^+ and K^-, respectively[9]. Similar to experimental data, the relative elliptic flow difference between π^+ and π^- is negative at all energies after including their potentials, although ours have smaller magnitudes. We have also found that, as seen in experiments[9], the relative v_2 difference between Λ hyperon and anti-Λ is smaller than that between p and anti-p, because the Λ (anti-Λ) potential is only 2/3 of the p (anti-p) potential.

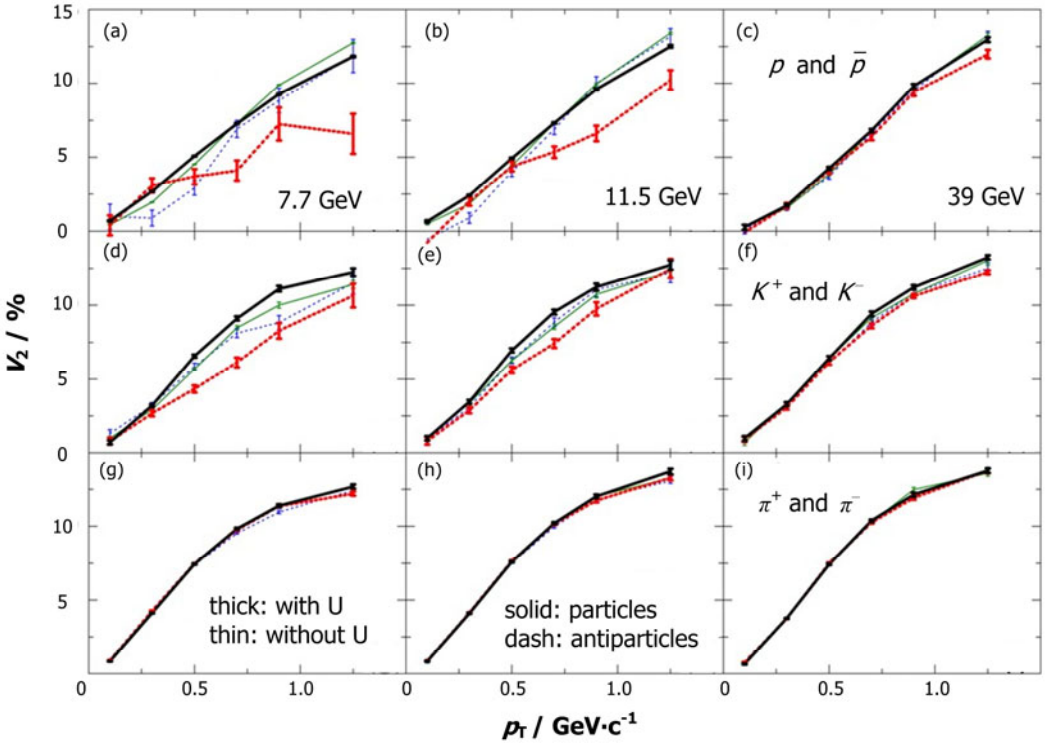

Fig.1 (Color online) Differential elliptic flows of mid-rapidity ($|y|<1$) p and anti-p [(a), (b), (c)], K^+ and K^- [(d)(e)(f)], and π^+ and π^- [(g)(h)(i)] with and without hadronic potentials in Au+Au collisions at b = 8 fm and center of mass energy of 7.7 GeV(a)(d)(g), 11.5 GeV(b)(e)(h), and 39 GeV (c)(f)(i) from the string melting AMPT model. The solid (dashed) curves represent the results of particles (anti-particles) while the thick (thin) curves represent the results with (without) potentials.

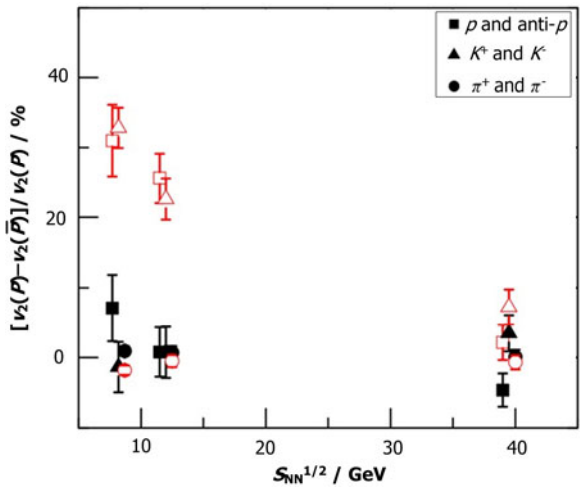

Fig.2 (Color online) Relative elliptic flow difference between mid-rapidity ($|y|<1$) p and anti-p, K^+ and K^-, and π^+ and π^- with (open symbols) and without (solid symbols) hadronic potentials in Au+Au collisions at b=8 fm and the center of mass energy of 7.7 GeV, 11.5 GeV and 39 GeV from the string melting AMPT model.

3 Partonic potentials and elliptic flows

3.1 Nambu-Jona-Lasinio model

To study the effect of partonic mean fields on parton elliptic flows, we have used in Ref.[14] the NJL model[39,40], particularly the one for three quark flavors[7]. Like particles and antipartcles in baryon-rich hadronic matter, quarks are affected by attractive scalar and repulsive vector fields, while antiquarks are affected by attractive scalar but attractive vector fields in baryon-rich quark matter. The value of the attractive scalar mean field is related to the difference between the current and the constituent quark masses, which has a maximum value of about –300 MeV. The magnitude of vector mean field depends on the product of the quark vector coupling and the net-baryon density. For the vector coupling $g_V \approx 17$ MeV fm^3 obtained from the Fierz transformation of the quark scalar interaction in the NJL Lagrangian and used in calculating the results shown in Figs.3 and 4 of Section 3, the vector mean field has a magnitude of ≈17 MeV if the net-baryon density is 1 fm^{-3}, leading to a difference of ≈34 MeV in the quark and antiquark vector mean fields.

Similar to that for the hadronic matter[41,42], the time evolution of the partonic matter produced in relativistic heavy ion collisions can be described by the transport equation for the parton phase-space distribution function.

3.2 Quark and antiquark elliptic flows

For the initial quark and antiquark rapidity and transverse momentum distributions in Au+Au collisions at center of mass energy of 7.7 GeV and at impact parameter b=8 fm, we use the valence quarks and antiquarks converted from hadrons that are obtained from the HIJNIJ model[43] through the Lund string fragmentation as implemented in the AMPT model with string melting[16]. Including partonic mean fields and using a constant isotropic parton scattering cross section of 5 mb, we have solved the partonic transport equation with the test particle method[44]. Figure 3 shows the transverse momentum dependence of quark and antiquark elliptic flows at the end of the partonic phase, which is about 1.9 fm/c after the start of the partonic evolution when the energy density in the center of produced quark matter decreases to 0.8 GeV/fm^3. Shown are the four cases of including only scalar mean field, scalar and time-component vector mean fields, scalar and space-component vector mean fields, and scalar and full vector mean fields. For the scalar mean field, which is attractive for both quarks and antiquarks, it leads to a similar reduction of the quark and antiquark elliptic flow as first found in Ref.[45]. The vector mean field, on the other hand, has very different effects on quarks and antiquarks in the baryon-rich QGP as it is repulsive for quarks and attractive for antiquarks. The time component of vector mean field turns out to have the strongest effect, resulting in a significant splitting of the quark and antiquark elliptic flows as a result of enhanced quark elliptic flow and suppressed antiquark elliptic flow. The space component of vector mean field has, however, an opposite effect; it suppresses the elliptic flow of quarks and enhances that of antiquarks, although relatively small and appearing later in the partonic stage compared to that of the time component of vector mean field.

For the case including the scalar and both components of vector mean field, the difference between the integrated elliptic flow of up and down quarks and their antiquarks is about 60% of the integrated elliptic flow of up and down quarks, and that between strange quarks and anti-strange quarks is about 29% of the integrated elliptic flow of strange quarks.

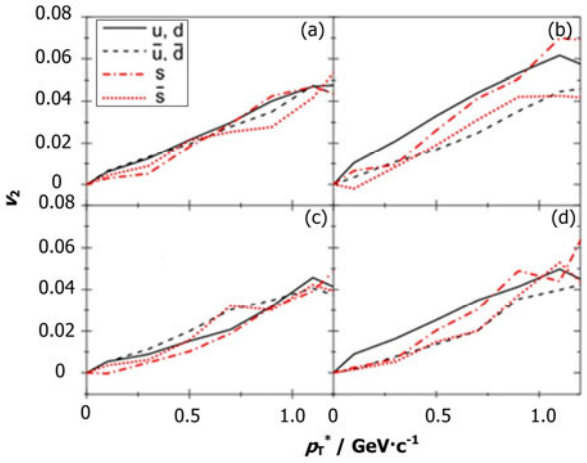

Fig.3 (Color online)Elliptic flows of light and strange quarks and antiquarks at midrapidity ($|y|$<1) as functions of transverse momentum at hadronization for the cases of including only scalar mean field (S) (a), scalar and time-component vector mean fields (S+V_0) (b), scalar and space-component vector mean fields (S+V_i) (c), and scalar and full vector mean fields (S+V_0+V_i) (d).

3.3 Hadronic elliptic flows

To study how different quark and antiquark elliptic flows are reflected in those of produced hadrons, we have used the coalescence model to convert them to hadrons at hadronization[46]. In this model, the probability for a quark and an antiquark to form a meson is proportional to the quark Wigner function of the meson with the proportional constant given by the statistical factor for colored spin-1/2 quark and antiquark to form a colorless meson[47,48].The probability for three quarks or antiquarks to coalesce to a baryon or an anti-baryon is similarly proportional to the quark Wigner function of the baryon. Since π^+ and π^- elliptic flows are affected similarly by the partonic mean fields as a result of similar elliptic flows for u and d quarks and their antiquarks, we have considered only p, K, and Λ and their antiparticles.

In Fig.4, we show by solid and dashed lines, respectively, the elliptic flows of p and anti-p (left panel), Λ and anti-Λ (middle panel), and K^+ and K^- (right panel), at hadronization as functions of transverse momentum. It is seen that the quark coalescence leads to a larger hadron elliptic flow than the quark elliptic flow at same transverse momentum. Furthermore, the elliptic flows of p, Λ, and K^- are

respectively larger than those of anti-p, anti-Λ, and K^+, leading to the relative differences between their integrated elliptic flows of about 45, 40, and –6.0%, respectively, as shown by solid symbols in Fig.5 for the quark vector coupling g_V = 17 MeV fm^3, compared with 63±14, 54±27, and 13±2% measured in experiments shown by open symbols in the left side of Fig.5.

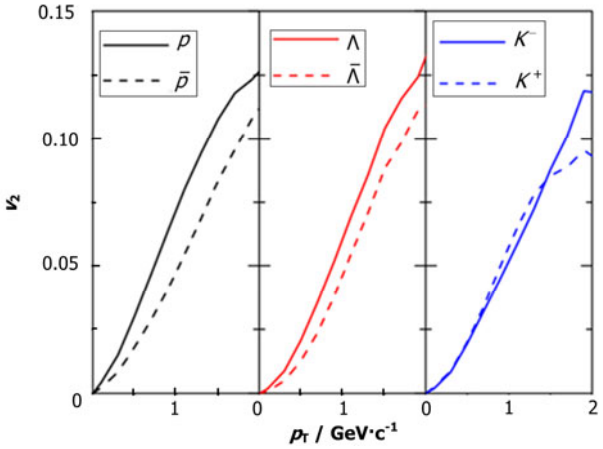

Fig.4 (Color online) Elliptic flows of mid-rapidity ($|y|$<1) p and anti-p (left panel), Λ and anti-Λ (middle panel), and K^+ and K^- (right panel), at hadronization as functions of transverse momentum.

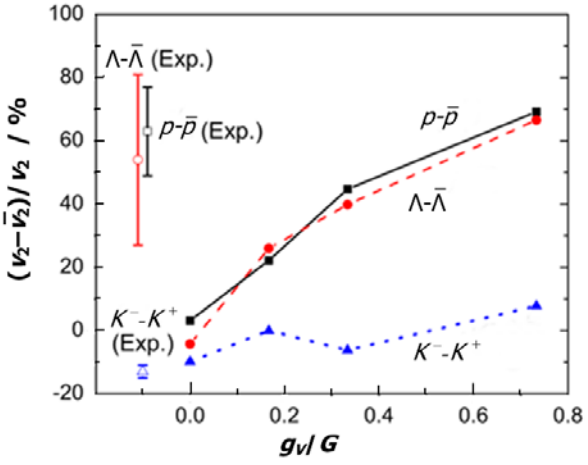

Fig.5 (Color online) Relative difference between integrated elliptic flow of mid-rapidity ($|y|$<1) p and anti-p (solid squares), Λ and anti-Λ (solid circles), and K^+ and K^- (solid triangles) at hadronization for several values of quark isoscalar vector coupling. Experimental data from Refs.[8,9] are shown by open symbols in the left side.

The dependence of the relative difference between integrated particle and antiparticle elliptic flows on the vector coupling g_V is shown in Fig.5. Besides the value g_V/G=0.33, corresponding to g_V=17 MeV fm^3, two other values of 0.165 and 0.73[49] are also used. The relative integrated elliptic flow differences are seen to increase almost linearly with the strength of the vector coupling.

4 Conclusion

We have studied the elliptic flows of p, K^+, π^+ and their antiparticles in heavy ion collisions at BES energies by extending the string melting AMPT model to include their mean-field potentials in the hadronic stage[13]. Because of the more attractive anti-p than p potentials, the attractive K^- and repulsive K^+ potentials, and the slightly attractive π^+ and repulsive π^- potentials in the baryon- and neutron-rich matter formed in these collisions, smaller elliptic flows are obtained for anti-p, K^-, and π^+ than for p, K^+, and π^-. Also, the differences between the elliptic flows of particles and their antiparticles are found to decrease with increasing collision energy as a result of decreasing baryon chemical potential of produced hadronic matter. Although our results are qualitatively consistent with the experimental observations, they somewhat underestimate the relative elliptic flow difference between p and anti-p as well as that between π^- and π^+ and overestimate that between K^+ and K^-.

We have also studied the effect of partonic mean fields on the elliptic flows of quarks and antiquarks in a baryon-rich quark matter by using a transport model based on the NJL model[14]. Although the scalar mean field, which is attractive for both quarks and antiquarks, leads to a similar reduction of the quark and antiquark elliptic flow, the vector mean field, on the other hand, results in a significant splitting of the quark and antiquark elliptic flows as a result of enhanced quark elliptic flow and suppressed antiquark elliptic flow. Using the quark coalescence model, we have further studied the elliptic flows of p, Λ, and K^+ and their antiparticles produced from the baryon-rich quark matter and found that the differences between particle and antiparticle elliptic flows are appreciable as a result of the different quark and antiquark elliptic flows. The magnitude of the relative integrated elliptic flow difference between particles and their antiparticles depends on the strength of the vector coupling. For the small vector coupling obtained from the Fierz transformation of the scalar

interaction in the NJL model (g_v/G=0.33), the relative elliptic flow difference due to partonic mean fields is about one third larger for p and anti-p, close to a factor of two larger for Λ and anti-Λ, and about a factor of five smaller but with an opposite sign for K^+ and K^-, compared to corresponding values due to the effect of hadronic potentials given in Ref.[13].

As to the elliptic flows of π^+ and π^-, they are the same in our study reported in Ref.[14] as we have not included the isovector part of partonic mean fields. As shown in our study reported in Ref.[13], including the isovector hadronic mean fields indeed leads to a splitting of the elliptic flow of π^+ and π^-, although a factor of five smaller than the measured value. It is thus of great interest to study the effect of quark isovector mean field on the π^+ and π^- difference and compare it with that due to the chiral magnetic effect suggested in Ref.[12].

If the effects of partonic and hadronic mean-field potentials were additive, which certainly needs to be checked in future studies, then the final relative elliptic flow differences between p and anti-p, Λ and anti-Λ, and K^+ and K^- would be close to those measured in the BES experiments at RHIC if a small quark vector coupling is used. The latter is consistent with that extracted in Refs.[50-52] from the baryon number susceptibilities measured in lattice QCD. A more quantitative study that includes both partonic and hadronic mean-field effects as well as the chemical reactions in the partonic phase thus provides the possibility of extracting information on the strength of quark vector interaction in baryon-rich QGP and thus its equation of state from the BES program at RHIC.

References

1 Bazavov A, Bhattacharya T, Cheng M, *et al.* Phys Rev D, 2012, **85:** 054503.

2 Bernard C, Burch T, DeTar C, *et al.* Phys Rev D, 2005, **71:** 034504.

3 Aoki Y, Endrő di G, Fodor Z, *et al.* Nature 2006, **443:** 675–678.

4 Asakawa M and Yazaki K. Nucl Phys A, 1989, **504:** 668–684.

5 Fukushima K. Phys Rev D, 2008, **77:** 114028.

6 Carignano S, Nickel D, Buballa M. Phys Rev D, 2010, **82:** 054009.

7 Bratovie N M, Hatsuda T, Weise W. arXiv:1204.3788 [hep-ph].

8 Kumar L. J Phys G, 2011, **38:** 124145.

9 Mohanty B. J Phys G, 2011, **38:** 124023.

10 Greco V, Mitrovski M, Torrieri G. Phys Rev C, 2012, **86:** 044095.

11 Dunlop J C, Lisa M A, Sorensen P. Phys Rev C, 2011, **84:** 044914.

12 Burnier Y, Kharzeev D E, Liao J, *et al.* Phys Rev Lett, 2011, **107:** 052303.

13 Xu J, Chen L W, Ko C M, *et al.* Phys Rev C, 2012, **85:** 041901.

14 Song T, Plumari S, Greco V, *et al.* arXiv:1211.5511 [nuc-th].

15 Steinheimer J, Koch V, Bleicher M. Phys Rev C, 2012, **86:** 044903.

16 Lin Z W, Ko C M, Li B A, *et al.* Phys Rev C, 2005, **72:** 064901.

17 Wang X N and Gyulassy M. Phys Rev D, 1991, **44:** 3501–3516.

18 Zhang B. Comp Phys Comm, 1998, **109:** 193–206.

19 Andronic A, Braun-Munzinger P, Stachel J. Nucl Phys A, 2010, **834:** 237c–240c.

20 Li B A and Ko C M. Phys Rev C, 1995, **52:** 2037–2063.

21 Danielewicz P, Lacey R, Lynch W G. Science, 2002, **298:** 1592–1596.

22 Ko C M and Li G Q. J Phys G, 1996, **22:** 1673–1725.

23 Ko C M, Koch V, Li G Q. Ann Rev Nucl Part Sci, 1997, **47:** 505–539.

24 Li G Q, Ko C M, Fang X S, *et al.* Phys Rev C, 1994, **49:** 1139–1148.

25 Li G Q, Lee C H, Brown G E. Phys Rev Lett, 1997, **79:** 5214–5217; Nucl Phys A, 1997, **625:** 372–434.

26 Kaiser N and Weise W. Phys Lett B, 2001, **512:** 283–289.

27 Gaitanos T, Kaskulov M, Lenske H. Phys Lett B, 2011, **703:** 193–198.

28 Barnes P D, Dytman S, Eisenstein R A, *et al.* Phys Rev Lett, 1972, **29:** 1132–1134.

29 Poth H, Backenstoss G, Bergström I, *et al.* Nucl Phys A, 1978, **294:** 435–449.

30 Batty C J. Nucl Phys A, 1981, **372:** 433–444.

31 Wong C Y, Kerman A K, Satchler G R, *et al.* Phys Rev C, 1984, **29:** 574–580.

32 Janouin S, Lemaire M C, Garreta D, *et al.* Nucl Phys A, 1986, **451:** 541–772.

33 Friedman E, Gal A, Batty C J. Nucl Phys A, 1994, **579:** 518–538.

34 Friedman E, Gal A, Mareš J. Nucl Phys A, 2005, **761:** 283–295.

35 Bratkovskaya E L, Cassing W, Mosel U. Nucl Phys A, 1997, **622:** 593–604.

36 Sibirtsev A and Cassing W. Nucl Phys A, 1998, **641:** 476–498.

37 Friedman E, Gal A, Mareš J, *et al.* Phys Rev C, 1999, **60:** 024314.

38 Song G, Li B A, Ko C M. Nucl Phys A, 1999, **646:** 481–499.

39 Nambu Y and Jona-Lasinio G. Phys Rev, 1961, **122:** 345–358.

40 Nambu Y and Jona-Lasinio G. Phys Rev, 1961, **124:** 246–254.

41 Ko C M, Li Q, Wang R C. Phys Rev Lett, 1987, **59:** 1084–1087.

42 Ko C M and Li Q. Phys Rev C, 1988, **37:** 2270–2273.

43 Gyulassy M and Wang X N. Comp Phys Comm, 1994, **83:** 307–331.

44 Abada A and Aichelin J. Phys Rev Lett, 1995, **74:**3130–3133.

45 Plumari S, Baran V, Di Tor M, *et al.* Phys Lett B, 2010, **689:** 18–22.

46 Chen L W, Ko C M, Li B A. Phys Rev C, 2003, **68:** 017601; Nucl Phys A, 2003, **729:** 809–834.

47 Greco V, Ko C M, Lévai P. Phys Rev Lett, 2003, **90:** 202302; Phys Rev C, 2003, **68:** 034904.

48 Greco V, Ko C M, Rapp R. Phys Lett B, 2004, **595:** 202–208.

49 Lutz M, Klimt S, Weise W. Nucl Phys A, 1992, **542:** 521–558.

50 Kunihiro T. Phys Lett B, 1991, **271:** 395–402.

51 Ferroni L and Koch V. Phys Rev C, 2011, **83:** 045205.

52 Steimheimer J and Schramm S. Phys Lett B, 2011, **696:** 257–261.